Anal. Chem. **2003,** *75,* 6875−6885

Sample Metallization for Performance Improvement in Desorption/Ionization of Kilodalton Molecules: Quantitative Evaluation, Imaging Secondary Ion MS, and Laser Ablation

A. Delcorte,*,† J. Bour,‡ F. Aubriet,‡ J.-F. Muller,‡ and P. Bertrand†

Unité de Physico-Chimie et de Physique des Matériaux, Université catholique de Louvain, 1 Croix du Sud, B-1348, Louvain-la-Neuve, Belgium, and Laboratoire de Spectrométrie de Masse et de Chimie Laser, 1 Boulevard Arago, F-57078, Metz, France

The metallization procedure, proposed recently for signal improvement in organic secondary ion mass spectrometry (SIMS) (Delcorte, A.; Médard, N.; Bertrand, P. *Anal. Chem*. 2002, *74*, 4955)., has been thoroughly tested for a set of kilodalton molecules bearing various functional groups: Irganox 1010, polystyrene, polyalanine, and copper phthalocyanine. In addition to gold, we evaluate the effect of silver evaporation as a sample treatment prior to static SIMS analysis. Ion yields, damage cross sections, and emission efficiencies are compared for Ag- and Au-metallized molecular films, pristine coatings on silicon, and submonolayers of the same molecules adsorbed on silver and gold. The results are sample-dependent but as an example, the yield enhancement calculated for metallized Irganox films with respect to untreated coatings is larger than 2 orders of magnitude for the quasimolecular ion and a factor of 1−10 for characteristic fragments. Insights into the emission processes of quasimolecular ions from metallized surfaces are deduced from kinetic energy distribution measurements. The advantage of the method for imaging SIMS applications is illustrated by the study of a nonuniform coating of polystyrene oligomers on a 100-μm polypropylene film. The evaporated metal eliminates sample charging and allows us to obtain enhanced quality images of characteristic fragment ions as well as reasonably contrasted chemical mappings for cationized PS oligomers and large PP chain segments. Finally, we report on the benefit of using metal evaporation as a sample preparation procedure for laser ablation mass spectrometry. Our results show that the fingerprint spectra of Au-covered polystyrene, polypropylene, and Irganox films can be readily obtained under 337-nm irradiation, a wavelength for which the absorption of polyolefins is low. This is probably because the gold clusters embedded in the sample surface absorb and transfer the photon energy to the surrounding organic medium.

The performance of methods designed for the mass spectrometric analysis of organic samples is largely dependent on the specific routes used for sample preparation. In laser (MALDI) and kiloelectronvolt particle-induced desorption secondary ion mass spectrometry (SIMS), it has been clearly shown that the use of an appropriate substrate or matrix could greatly enhance the measured molecular ion yields. Although the mechanisms of matrix/substrate enhancement generally differ for the two types of interactions, it has been observed that some matrixes and substrates provide a drastic signal improvement with both techniques.[1,2]

Recently, we reported on gold metallization as a method to enhance secondary ion yields from organic samples, including polymers.[3] The procedure consists of the evaporation of minute quantities of metal on the sample surface.[4] The results, particularly impressive for thick polymeric samples and polymer additives, indicated that the signal improvement was most likely the result of a change in the ionization probability of the sputtered molecules and fragments. Beside the formation of gold adduct ions, the intensities of both positive and negative characteristic fragments were strongly enhanced, even for high molecular weight polyolefins. From those results, it was unlikely that the pronounced intensity increase could be only due to the migration of the considered molecules or molecular segments on top of the gold clusters or islands; a situation that would mimic the well-studied configuration of molecular overlayers adsorbed on metal substrates. Instead, we believe that the increase must be attributed in most cases to the modification of the electronic properties of the gold-covered surface, favoring ion formation via improved or additional charge-transfer mechanisms.

Prior to our article on gold metallization,[3] there had been other studies dealing with silver evaporation or sputtering as a sample preparation route for SIMS analysis.[5−10] Nevertheless, the assessment of the yield increase as well as the comparison between

* Corresponding author. Phone: 32-10-473582. Fax: 32-10-473452. E-mail: delcorte@pcpm.ucl.ac.be.

† Université catholique de Louvain.

‡ Laboratoire de Spectrométrie de Masse et de Chimie Laser.

(1) Wu, K. J.; Odom, R. W. *Anal. Chem*. **1996**, *68*, 873.
(2) Wittmaak, K.; Szymczak, W.; Hoheisel, G.; Tuszynski, W. *J. Am. Soc. Mass Spectrom*. **2000**, *11*, 553.
(3) Delcorte, A.; Médard, N.; Bertrand, P. *Anal. Chem*. **2002**, *74*, 4955.
(4) Travaly, Y.; Bertrand, P. *Surf. Interface Anal.* **1995**, *23*, 328.
(5) Linton, R. W.; Mawn, M. P.; Belu, A. M.; DeSimone, J. M.; Hunt, M. O. Jr.; Menceloglu, Y. Z.; Cramer, H. G.; Benninghoven, A. *Surf. Interface Anal.* **1993**, *20*, 991.

10.1021/ac0302105 CCC: $25.00
Published on Web 11/18/2003

several metals or with other sample preparation procedures is still incomplete today. In particular, a more detailed comparison between metallized films and submonolayers of molecules cast on metal substrates (a well-documented procedure[11−22]) would be useful, since both methods lead to molecule cationization. For applications, the metallization route appears potentially more powerful because it can be applied to any kind of surface, without the sample dilution and submonolayer deposition steps that strongly limit sample cationization by metal substrates. For example, via metal evaporation, biomolecules or additive molecules sitting on an organic or a polymeric surface might be detected intact, or with a much higher yield, through metal cationization. Finally, more insights into the physics underlying molecular ion emission from such metallized coatings are also desired.

The goals of this article, devoted to the analysis of kilodalton molecules, are 3-fold: first, to quantify the efficiency improvement provided by the metallization procedure for static SIMS analysis; second, to investigate the influence of the method for the molecular imaging of organic surfaces, including bulk, insulating polymers; third, to study the transferability of the metallization procedure to the sister desorption/ionization technique, laser ablation mass spectrometry. In laser ablation experiments, metal clusters located in the surface region should behave as photon absorbers, thereby providing another sort of matrix as those used for large molecule emission in traditional matrix-assisted laser desorption/ionization (MALDI[23,24]). Four molecules belonging to different chemical families (Irganox 1010, 1176 Da; polystyrene, 1000−3000 Da; polyalanine, 1000−5000 Da; and phthalocyanine 1120−1135 Da) have been chosen to specifically investigate the effect of sample metallization on the yields and properties of sputtered kilodalton molecular ions. The chosen metals are silver[25,26] and gold,[3] both known for their efficiency as cationizing agents.[27] The Results and Discussion section describes the mass spectra of the pristine and metallized molecular films, in comparison with submonolayers of the same species cast on metallic substrates. The yields and damage cross sections of metallized films are also investigated, and the yield enhancements and efficiencies obtained via metallization are compared to other sample preparation procedures. The emission mechanisms are briefly discussed on the basis of the kinetic energy distributions measured for metal-cationized molecular ions sputtered from submonolayers on metals and from metallized organic coatings. After demonstrating the advantage of metal evaporation for SIMS imaging applications, we finally discuss its use as a new sort of matrix for laser ablation experiments.

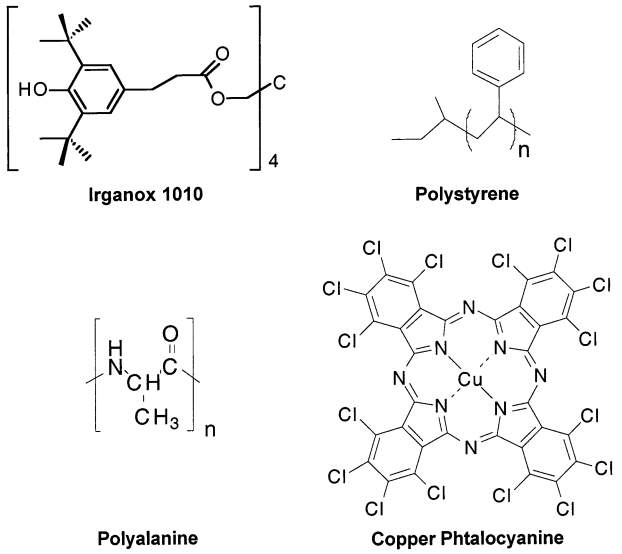

Figure 1. Molecular formulas of the kilodalton molecules under investigation.

MATERIALS AND METHODS

Samples. Four molecules with a mass above 1 kDa and including various functional groups have been selected for this study. These are Irganox 1010, low molecular weight polystyrene, poly-DL-alanine, and copper phthalocyanine. The chemical formulas of these compounds are shown in Figure 1. To obtain model samples of each of these substances, they were dissolved (1−10 mg/mL) and cast as films by depositing a droplet of the solution on a mirror-polished silicon substrate of ~1 cm^2. The solvent was then allowed to freely evaporate. The origin of the samples and the nature of the solvents are listed in Table 1. For comparison, molecular submonolayers on silver and gold substrates have been obtained by casting very dilute solutions (0.1 mg/mL) of the same molecules on silver foils and gold-metallized silicon wafers. The metallized substrates were prepared by first evaporating a 5-nm titanium adhesive layer and then a 100-nm gold layer on 1 cm^2

(6) Belu, A. M.; Mawn, M. P.; Linton, R. W. In *Secondary Ion Mass Spectrometry, SIMS IX Proceedings*; Benninghoven, A., Nihei, Y., Shimizu, R., Werner, H. W., Eds.; Wiley, New York, 1994; p 780.
(7) Karen, A.; Benninghoven, A. In *Secondary Ion Mass Spectrometry, SIMS IX Proceedings*; Benninghoven, A., Nihei, Y., Shimizu, R., Werner, H. W., Eds.; Wiley, New York, 1994; pp 788.
(8) Simon, C. Caractérisation de surfaces organiques moléculaires et polymères par SIMS statique. Ph.D. Thesis, University of Metz, 1996.
(9) Simon, C.; Saldi, F.; Migeon, H.-N. In *Polymer-Solid Interfaces*: *From Model to Real Systems*; Pireaux, J.-J., Delhalle, J., Rudolf, P., Eds.; Presses Universitaires de Namur, Namur, 1998; p 411.
(10) Yanashima, H.; Sado, M.; Minobe, M. In *Secondary Ion Mass Spectrometry, SIMS X Proceedings*; Benninghoven, A., Hagenhoff, B., Werner, H. W., Eds.; Wiley, New York, 1997; p 751.
(11) Grade, H.; Winograd, N.; Cooks, R. G. *J. Am. Chem. Soc.* **1977**, *99*, 7725.
(12) Grade, H.; Cooks, R. G. *J. Am. Chem. Soc.* **1978**, *100*, 5615.
(13) Bletsos, I. V.; Hercules, D. M.; van Leyen, D.; Benninghoven, A. *Macromolecules* **1987**, *20*, 407.
(14) Bletsos, I. V.; Hercules, D. M.; van Leyen, D.; Hagenhoff, B.; Niehuis, E.; Benninghoven, A. *Anal. Chem.* **1991**, *63*, 1953.
(15) Zimmerman, P. A.; Hercules, D. M.; Benninghoven, A. *Anal. Chem.* **1993**, *65*, 983.
(16) Benninghoven, A.; Hagenhoff, B.; Niehuis, E. *Anal. Chem.* **1993**, *65*, 630A.
(17) Benninghoven, A. *Surf. Sci.* **1994**, *299/300*, 246.
(18) Xu, K.; Proctor, A.; Hercules, D. M. *Mikrochim. Acta* **1996**, *122*, 1.
(19) Nicola, A. J.; Muddiman, D. C.; Hercules, D. M. *J. Am. Soc. Mass Spectrom.* **1996**, *7*, 467.
(20) Pleul, D. Simon, F.; Jacobasch, H.-J. *Fresenius J. Anal. Chem.* **1997**, *357*, 684.
(21) Gusev, A. I.; Choi, B. K.; Hercules, D. M. *J. Mass Spectrom.* **1998**, *33*, 480.
(22) Keller, B. A.; Hug, P. In *Secondary Ion Mass Spectrometry, SIMS XII* Proceedings; Benninghoven, A., Bertrand, P., Migeon, H.-N., Werner, H. W., Eds.; Elsevier: Amsterdam, 2000; pp 749, 885.
(23) Tanaka, K.; Waki, H.; Ido, Y.; Akita, S.; Yoshida, Y.; Yoshida, T. *Rapid Commun. Mass Spectrom.* **1988**, *2*, 151.
(24) Karas, M.; Bachmann, D.; Bahr, U.; Hillenkamp, F. *Int. J. Mass Spectrom. Ion Processes* **1988**, *78*, 53.
(25) Ruch, D.; Boes, C.; Zimmer, R.; Muller, J.-F.; Migeon, H.-N. *Appl. Surf. Sci.* **2003**, *203−204*, 566.
(26) Ruch, D.; Muller, J.-F.; Migeon, H.-N.; Boes, C.; Zimmer, R. *J. Mass Spectrom.* **2003**, *38*, 50.
(27) Delcorte, A.; Wojciechowski, I.; Gonze, X.; Garrison, B. J.; Bertrand, P. *Int. J. Mass Spectrom.* **2002**, *214*, 213.

Table 1. Origin of the Organic Samples and Nature of the Solvents Used in the Experiments

	origin	solvent
Irganox 1010	Ciba	cyclohexane
polystyrene	Scientific Polymer Products	toluene
poly(DL-alanine)	Sigma-Aldrich	water
copper phthalocyanine	Clarian	chloroform

silicon wafers. Conversely, the organic samples cast on clean silicon wafers, as well as the bulk polymers, were metallized afterward, by evaporating 20 nmol of silver (gold)/cm^2 on their top surface. This amount was shown to be the optimum with respect to secondary ion yield enhancement in the case of gold-metallized polystyrene oligomer films.[3] Prior to organic sample deposition/gold metallization, all the silicon substrates were rinsed in 2-propanol and hexane (p.a. grade; Vel).

The evaporation was carried out in an Edwards evaporator at an operating pressure of $\sim 10^{-6}$ mbar and a deposition rate of 0.1 nm/s. The deposited metal amount was measured with a quartz crystal monitor, and the given values correspond to the assumption that the sticking coefficient was the same on the monitor and the organic samples. Because of this hypothesis, the deposited amount might be overestimated[28] and the quoted metal quantities provided along the article must be considered as indicative rather than accurate values. Despite this uncertainty, the deposition conditions are reproducible, which validates the method.

Secondary Ion Mass Spectrometry. The secondary ion mass analyses and images, the degradation studies and the kinetic energy distribution (KED) measurements were performed in a Phi-Evans time-of-flight (TOF) SIMS (TRIFT 1) using a 15-keV Ga^+ beam (FEI 83-2 liquid metal ion source, ~550-pA dc current, 22-ns pulse width bunched down to ~1 ns, and 5-kHz repetition rate for the mass range 0−5 kDa).[29] The experimental setup has been described in detail elsewhere.[30] Except for the degradation and KED measurements, the TOF-SIMS analyses were obtained by collecting the secondary ion signal in the mass range $0 < m/z < 5000$ for the 600-s bombardment of a 180 × 180 μm^2 sample area, which corresponds to a fluence of 3.5×10^{11} ions/cm^2. To improve the measured intensities, the secondary ions were postaccelerated by a high voltage (7 kV) in front of the detector. In the discussion, all the quoted secondary ion intensities and yields (number of detected secondary ions per primary ion) are based on calculated peak areas.

TOF-SIMS images were obtained by rastering the 15-keV Ga^+ beam for 1800 s over a surface area of either 120 × 120 μm^2 (metallized sample) or 180 × 180 μm^2 (pristine sample), i.e., with a primary ion fluence of 2.3×10^{12} ions/cm^2 or, respectively, 10^{12} ions/cm^2.

To measure energy spectra, the secondary ions were energy selected at the crossover following the first ESA, where the energy dispersion is maximum, by a slit of 100-μm width (corresponding to a passband of 1.5 eV). The acquisition of mass spectra for different sample voltages allowed us to collect the signal corresponding to different energy windows of the KED. A 1-V increase of the sample potential corresponds to a 1-eV decrease in the KED. To reduce surface degradation,[31] several sets of measurements were conducted on different sample areas for each KED. For successive bombardment periods on the same sample area, the measured intensities were corrected using the degradation laws of the corresponding ions.[32] The zero of energy scale for each set was estimated from the intersection between the tangent to the increasing part of the KED of atomic ions and the energy axis. The corrected value of the sample voltage, giving the initial kinetic energy of the secondary ions, is called "apparent energy" in the presentation of the results.

Laser Ablation Mass Spectrometry (LAMS). The laser ablation mass spectra were performed with a Bruker Reflex IV Maldi-ToF instrument (Bruker-Franzen Analytik GmbH, Bremen, Germany) equipped with a delayed extraction. Ionization was achieved by using a nitrogen laser ($\lambda = 337$ nm, pulse duration 3 ns, output energy 400 μJ, repetition rate 5 Hz). The laser diameter was ~30 μm. The laser fluence may be varied by means of an attenuator from 22 to 540 mJ/cm^2. It was typically kept in our experiments at 75 mJ/cm^2. The mass spectrometer was operated in the reflectron mode at a total acceleration voltage of 20 kV and a reflecting voltage of 23 kV. A delay time of 400 ns was used prior to ion extraction. The obtained mass spectra were the result of the accumulation of tens of laser shots on different places of the same sample and were acquired in the 0−3500-kDa mass range. The ion assignment was attained after external calibration performed with poly(ethylene glycol) 600 or 1500 Na^+ and K^+ cationized ions. The two spectra presented hereafter are from raw data with no baseline correction and no signal smoothing.

RESULTS AND DISCUSSION

The first section compares the mass spectra, ion yields, damage cross sections, and emission efficiencies observed for pristine samples, metallized samples, and samples cast as a submonolayer on a metallic substrate. The application of the metallization procedure for SIMS imaging is treated in the second section, with the case study of a nonuniform coating of polystyrene (PS) oligomers on a biaxially stretched polypropylene (PP) film. In the third section, we investigate the use of metal evaporation as a sample preparation procedure for LAMS analysis.

Efficiency and Fundamentals of Molecular Ion Emission. (1) Irganox 1010. The molecular ion regions of the mass spectra of Irganox samples prepared using various procedures are displayed in Figure 2. The first two frames show the negative and positive mass spectra of the pristine molecular film. Silicon-related peaks could not be found on these spectra, indicating that the coating is thick enough to prevent substrate ion emission. The molecular ion of Irganox is dominant in the negative mode (frame 1) but very weak (~25−30 counts) in the positive mode (frame 2). Instead, there is a series of large characteristic fragments below $m/z = 900$. In particular, the cation at $m/z = 900$ is formed by the loss of one of the "repeat units" ($C_{17}H_{25}O_3$) from the pristine

(28) Novak, S.; Mauron, R.; Dietler, G.; Schlapbach, L. In *Metallized Plastics 2: Fundamental and Applied Aspects*; Mittal, K. L., Ed.; Plenum Press: New York, 1991; p 233.
(29) Schueler, B. W. *Microsc. Microanal. Microstruct.* **1992**, *3*, 119.
(30) Delcorte, A.; Vanden Eynde, X.; Bertrand, P.; Reich, D. F. *Int. J. Mass Spectrom.* **1999**, *189*, 133.
(31) Delcorte, A.; Weng, L. T.: Bertrand, P. *Nucl. Instrum. Methods Phys. Res. B* **1995**, *100*, 213.
(32) Arezki, B.; Delcorte, A.; Bertrand, P.; *Nucl. Instrum. Methods Phys. Res. B* **2002**, *193*, 755.

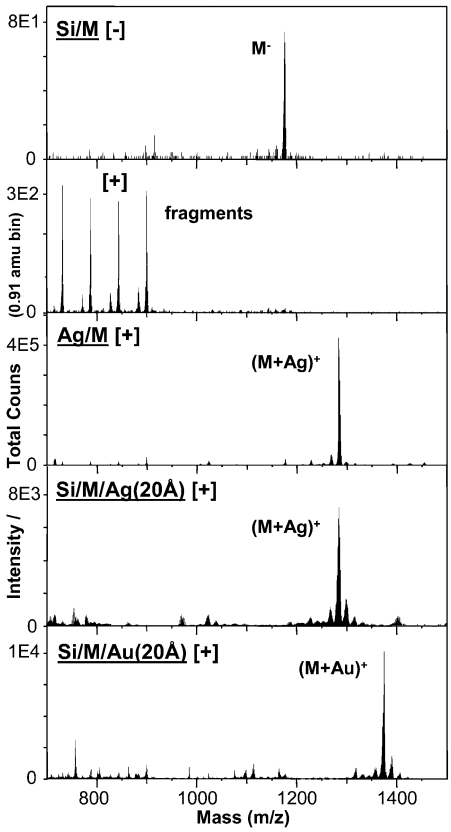

Figure 2. High-mass range of the secondary ion mass spectra of Irganox 1010 obtained via several sample preparation procedures. Frames 1 and 2, negative and positive mass spectra of the molecule cast on Si; frame 3, positive mass spectrum of the molecule cast as a submonolayer on Ag; frames 4 and 5, Ag- and Au-metallized (20 nmol/cm^2) coatings of Irganox on Si.

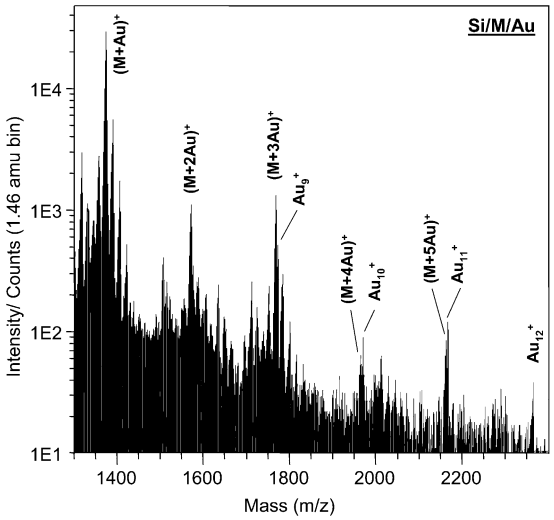

Figure 3. Mass distribution of the main gold molecule clusters sputtered from a Au-metallized (20 nmol/cm^2) Irganox 1010 coating on Si.

Table 2. Secondary Ion Yields (Y, Number of Detected Secondary Ions per Primary Ion) and Yield Enhancements Measured for Irganox Fragment and (Quasi)Molecular Ions[a]

	$C_4H_9O^+$		$C_{15}H_{23}O^+$		M^+		$(M + Me)^+$	
	Y (10^{-2})	E	Y (10^{-2})	E	Y (10^{-6})	E	Y (10^{-4})	E*
Si/M	1.7	1.0	1.9	1.0	1.5	1	0.0	0.0
Ag/M	12	7.2	19	9.7	1953	1318	443	29885
Au/M	4.0	2.3	4.8	2.4	20	13	1.8	125
Si/M/Ag	13	7.8	1.8	0.9	8.3	5.6	6.6	447
Si/M/Au	8.9	5.2	6.7	3.5	47	32	9.8	661

[a] Yield enhancement is defined as the measured ion yield for the considered sample divided by the ion yield obtained for the pristine organic layer cast on silicon ($E = Y/Y_{Si/M}$). In the last column, the enhancement (E*) is defined as the yield of metal-cationized molecules divided by the yield of molecular ions measured for the nonmetallized layer on Si. M indicates the entire Irganox molecule and Me the metal atom.

Irganox molecule. The positive mass spectrum obtained for the overlayer on Ag is displayed in frame 3, and those corresponding to the Ag and Au-metallized coatings are in the two bottom frames. In these three cases, the dominant peak is the metal-cationized Irganox molecule. From the molecular peak observed in the negative spectrum of the pristine sample to the cationized peak corresponding to the submonolayer on silver, the intensity scale varies over more than 3 orders of magnitude. This illustrates the signal enhancement provided by the cationization process. In addition, the high-mass range of the mass spectrum of Au-metallized Irganox indicates the presence of larger gold molecule clusters containing up to five gold atoms (Figure 3). These clusters constitute additional characteristic peaks of Irganox that can be used for chemical diagnostic. Their emission process is considered in the section below, Ion Kinetic Energies and Emission Mechanisms.

The useful yields—defined as the numbers of detected secondary ions per primary ion—of two fragment ions and the (cationized) molecular ion of Irganox are listed in Table 2. As an example, the intensity of the molecular ion is multiplied by a factor of 32 when the sample is metallized with gold. If one considers the Au-cationized molecular ion instead of the actual molecular ion for the metallized sample (last column), the multiplying factor is 661. Even though the exact mechanism remains unclear, the metal clusters sitting on the surface of the organic coating constitute a matrix that contributes to enhance the desorption−ionization yield of Irganox secondary ions. Beside the molecular ion signal enhancement related to the cationization process, there is also a noticeable intensity increase for characteristic fragment ions, which varies as a function of the considered fragments. In the case of gold metallization, the increase reaches a factor of 5.2 for $C_4H_9^+$ ($m/z = 57$) and 3.5 for $C_{15}H_{23}O^+$ ($m/z = 219$).

(2) Polystyrene. The mass spectra of polystyrene oligomers, either metallized with gold or adsorbed as a submonolayer on silver and gold and obtained in the same experimental conditions, have been presented elsewhere.[3] For the sake of conciseness, they are only briefly discussed with respect to ion yields in this article. Nevertheless, it is important to mention that the distribution of cationized oligomers is present in all the mass spectra, except of course for polystyrene cast on silicon and analyzed without further treatment.

The yield of the $C_7H_7^+$ fragment, of the cationized 16-mer and of the cationized 25-mer sputtered from coatings of low-mass polystyrene ($M_w = 2360$: $M_n = 2180$) are listed in Table 3. In this case, the results show that Au metallization induces a larger yield of fragments and cationized molecules than Ag metallization.

Table 3. Secondary Ion Yields (*Y*) and Yield Enhancements (*E*) Measured for Polystyrene Fragment and (Quasi)Molecular Ions[a]

	$C_7H_7^+$		(a) $(PS16+Me)^+$	(b) $(PS25+Me)^+$	
	Y (10^{-2})	E	Y (10^{-4})	Y (10^{-4})	(a)/(b)
Si/M	0.7	1.0	0.0	0.0	
Ag/M	11	15	57	26	2.2
Au/M	16	22	62	34	1.8
Si/M/Ag	2.9	4.0	5.3	0.7	7.6
Si/M/Au	6.0	8.1	14	2.5	5.4

[a] PS16 and PS25 are, respectively, the 16-mer and the 25-mer of polystyrene.

In comparison, the yields measured for submonolayers of PS oligomers cast on silver and gold are similar and more than 2 times greater than those corresponding to the metallized films. The shape of the oligomer distribution also changes significantly, as indicated by the ratio between the 16-mer and the 25-mer yields. For molecules cast on silver and gold, this ratio is close to 2, while it is larger than 5 in the case of metallized surfaces. Therefore, the average molecular weights obtained from the peak distributions of the metallized sample spectra will be lower than that calculated using submonolayers on metal and, in this example, farther from the chromatographic values.

(3) Damage Cross Sections and Efficiencies. Another method to determine the absolute yield enhancement for a given sample is by taking into account the resilience of the signal with increasing primary ion fluence. For this purpose, one should consider the time integral of the molecular ion signal until extinction rather than the instantaneous intensity measured in the static regime. The practical justification of this method is that, for numerous applications (e.g., SIMS imaging), the molecular signal needs to be maximized at all costs, including the loss of the static regime. Rather than systematically measuring the integral of the signal, the efficiency, ϵ, is defined as the ratio between the yield obtained in the static regime, Y, and the damage cross section, σ, of the probed molecular ion.[33]

The decay of the (cationized) molecular signal of Irganox and polystyrene as a function of the primary ion fluence is shown in Figure 4. In most cases, the decay curves can be fit by an exponential function, allowing us to extract a value for the damage cross section. The curve corresponding to the Ag-cationized PS 16-mers sputtered from a metallized film (Si/M/Ag) exhibits a change of slope after 10^{13} ions/cm^2. In that case, the value of σ is calculated on the basis of the exponential decay observed before 10^{13} ions/ cm^2. As summarized in Table 4, all the σ values are in the same range, between 2×10^{-13} and 5×10^{-13} cm^2. The fastest decay (highest σ) corresponds to the submonolayer of PS on Ag and the slowest decay (lowest σ) to the Au-metallized surfaces.

Table 4 lists the molecular ion efficiencies calculated from the measured yields and damage cross sections. For Irganox, there is more than 3 orders of magnitude between the lowest efficiency, corresponding to the molecule cast on silicon (Si/M), and the highest efficiency, obtained for the submonolayer on silver (Ag/M). With respect to the highest molecular ion intensity on silicon (negative spectrum), metallized samples also provide a significant efficiency enhancement, 1−2 orders of magnitude. For polystyrene, the efficiency increase provided by the silver substrate is not as dramatic. There is only a factor of 2.4 between the efficiencies calculated for the submonolayer on Ag and for the Au-metallized sample. The efficiencies obtained for Irganox and polystyrene molecules cast on silver are very different (1 order of magnitude). In contrast, the efficiencies seem to be much less dependent on the molecule nature using the metallization procedure. In addition, gold metallization proves to be slightly more efficient than silver metallization for both molecules.

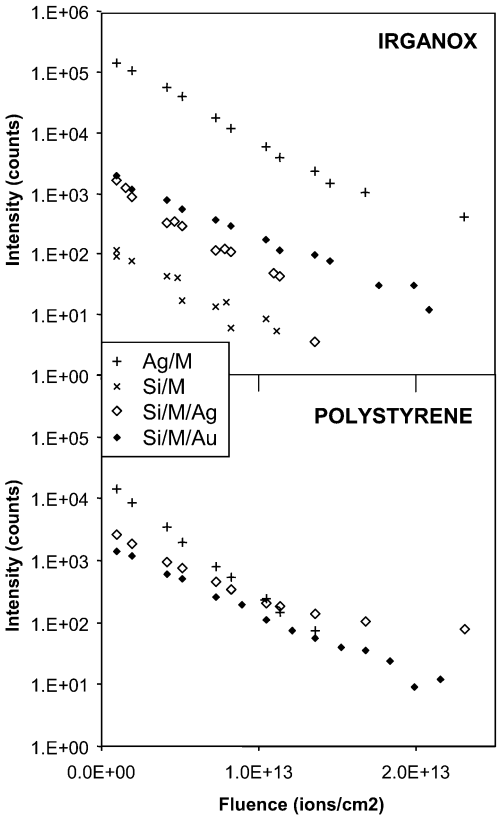

Figure 4. Degradation of the molecular ion signals as a function of the primary ion fluence for Irganox 1010 molecules and polystyrene oligomers obtained via several sample preparation procedures. Top frame, Irganox; bottom frame, polystyrene.

Table 4. Damage Cross Sections (σ) and Emission Efficiencies ($\epsilon = Y/\sigma$) of Quasimolecular Ions Sputtered from Irganox and Polystyrene Layers Elaborated Using Various Sample Preparation Procedures (See Text for Definitions)[a]

	Irganox		polystyrene	
	σ (10^{-13})	ϵ (Y/σ) (10^8)	σ (10^{-13})	ϵ (Y/σ) (10^8)
Si/M	3.51	0.84	n/a	n/a
Ag/M	3.45	1283	4.18	136
Si/M/Ag	3.14	21	2.43	22
Si/M/Au	2.37	41	2.35	57

[a] For the Si/M system, σ and ϵ were calculated using the molecular anion (negative spectrum).

(33) Van Stipdonk, M. J. In *ToF−SIMS: Surface Analysis by Mass Spectrometry*"; Vickerman, J. C., Briggs, D., Eds.; Surfacespectra/IMPublications: Chichester, U.K., 2001; p 316.

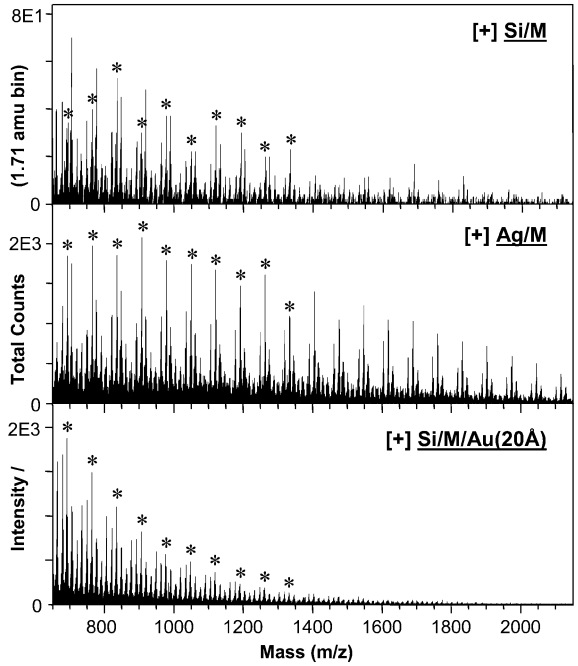

Figure 5. High-mass range of the secondary ion mass spectra of polyalanine. Frame 1, positive mass spectrum of the molecule cast on Si; frame 2, positive mass spectrum of the molecules cast as a submonolayer on Ag; frame 3, Au-metallized (20 nmol/cm^2) coating of polyalanine on Si.

(4) Polyalanine and Copper Phthalocyanine. The polyalanine sample used for this study is composed of oligomers with a mass below 5000 Da. Three partial mass spectra showing the high-mass cations sputtered respectively from the pristine sample cast on Si, from the sample deposited as a submonolayer on Ag, and from the Au-metallized coating are shown in Figure 5. All the spectra show the same series of ions, with different absolute and relative intensities. To guide the eye, successive peaks belonging to the most intense series for the Ag/M sample (second frame) are marked with a star on every spectrum. In a given series, the peaks are separated by 71 Da, i.e., the mass of the alanine repeat unit. Because they are present regardless of the preparation procedure, these peaks are not the result of cationization by a metal atom and no sign of such a process is detected in the rest of the mass spectrum. The mass-matching procedure indicates that the most intense series are probably due to $(M + Na)^+$ and $(M + K)^+$ (marked by stars), which is supported by the presence of relatively intense Na^+ and K^+ peaks in the low-mass range of the spectrum. Beside the absolute intensity variation, the distribution of peaks of the Au-metallized sample exhibits a different shape, with a quasi-exponential intensity decrease as a function of mass. The yields of fragments and molecular ions sputtered from polyalanine are reported in Table 5. In addition to the $C_2H_4N^+$ fragment ($m/z = 44$), we also report the intensity of the protonated alanine dimer ($m/z = 143$) and of two groups of peaks belonging to the series marked by a star and attributed to $(M + K)^+$ ions. ΣALA9$^+$ and ΣALA18$^+$ stand for the groups of peaks (exact mass, mass + 1, mass + 2, mass − 2) surrounding the cationized 9-mer and 18-mer of alanine. For these quasimolecular ions, the intensity enhancement provided by the metallization procedure is larger than 1 order of magnitude. The enhancement of the 9-mer intensity is similar in the case of the metallized samples and the sample cast as a submonolayer on silver. For the 18-mer, the intensity enhancement is larger than 2 orders of magnitude using a silver substrate. It is significantly lower on the metallized samples, which mirrors the different distribution shapes mentioned above. The shape of the metallized sample distribution, with a quasi-exponential intensity decay toward high masses, evokes previous results in which diffusion processes were predominant.[3] The intensity enhancement measured for the fragment ions, $C_2H_4N^+$ and the cationized alanine dimer, are essentially lower than 1 order of magnitude (except for the dimer in the Ag/M system).

The case of copper phthalocyanine is very specific because the pure molecule itself already contains a metallic atom, Cu. The positive mass spectra of pristine and metallized phthalocyanine coatings on Si are displayed in Figure 6. The signal corresponding to the intact molecule is split over a large range of masses, from 1120 to 1135 Da, with more intense peaks at odd masses, because of the isotopic distribution of the Cu atom and of the 16 Cl atoms present in the molecule. Relatively intense distributions of peaks at lower masses can be attributed to phthalocyanine molecules having lost one to four Cl atoms. A quick look at the metallized sample spectrum, bottom frame, indicates that the metallization

Table 5. Secondary Ion Yields (Y) and Yield Enhancements (E) Measured for Polyalanine Fragment and (Quasi)Molecular Ions[a]

	$C_2H_4N^+$		$(2ALA + H)^+$		ΣALA9$^+$		ΣALA18$^+$	
	Y (10^{-2})	E	Y (10^{-3})	E	Y (10^{-5})	E	Y (10^{-5})	E
Si/M	1.9	1.0	0.8	1.0	2.3	1.0	0.3	1.0
Ag/M	11	6.0	10	13	77	34	61	217
Si/M/Ag	10	5.6	2.7	3.5	60	26	18	62
Si/M/Au	5.6	3.0	1.7	2.2	67	29	6.2	22

[a] ALA stands for the alanine monomer. ΣALA9$^+$ and ΣALA18$^+$ correspond to the group of peaks surrounding, respectively, the cationized 9-mer and the cationized 18-mer of polyalanine (see text for details).

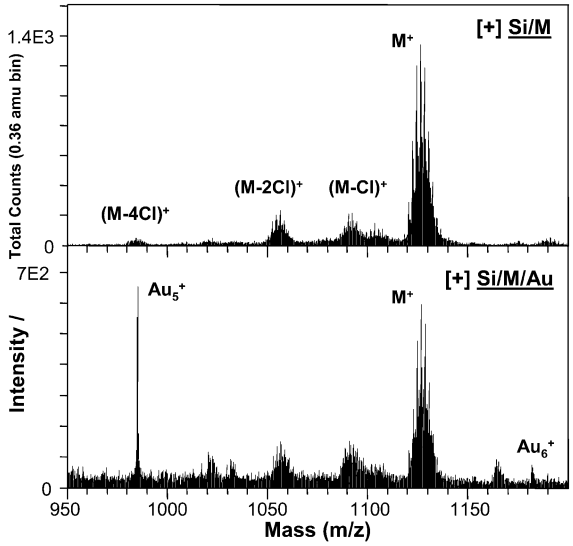

Figure 6. High-mass range of the secondary ion mass spectra of phthalocyanine. Top frame, positive mass spectrum of the molecules cast on Si; bottom frame, Au-metallized (20 nmol/cm^2) film of phthalocyanine on Si.

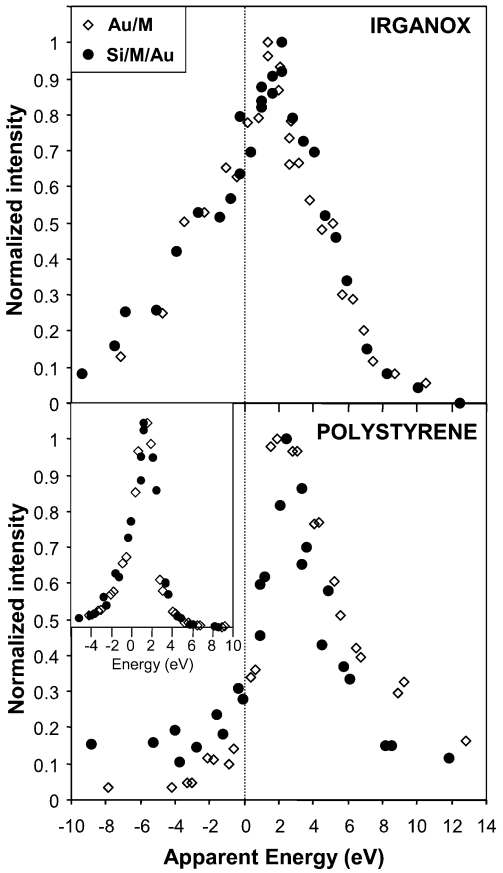

Figure 7. Kinetic energy distributions of Au-cationized Irganox 1010 molecules and PS oligomers desorbed from a film of organic sample covered by 20 nmol/cm^2 evaporated metal (full circles) and from a submonolayer of organic molecules cast on a gold substrate (open diamonds). The inset shows the energy spectra of $C_7H_7^+$ secondary ions sputtered from the same surfaces.

procedure does not induce any signal enhancement for phthalocyanine. The mass spectrum even appears noisier, and the peaks corresponding to the intact molecule are less intense. The cumulated yield of copper phthalocyanine molecular ions is 1.7 $\times$ 10^{-3} for the coating on Si and 0.8 $\times$ 10^{-3} for the Au-metallized coating. In addition, there is no Au-cationized molecule peak in the mass spectrum. The absence of positive effect of the metallization procedure on the molecular ion intensity is probably due to the fact that the pristine sample contains a metallic atom. This copper atom plays the role of the cationizing agent, as indicated by the high molecular ion yield measured for the untreated coating.

(5) Ion Kinetic Energies and Emission Mechanisms. A remarkable advantage of the metallization procedure for SIMS analyses is that the metal coating suppresses the need of a charge compensation setup (especially useful for thick organic samples). In turn, the stability of the surface potential under analysis allows us to measure the kinetic energy spectra of the sputtered species. The energy distributions of the Au-cationized Irganox and PS 16-mer molecules sputtered from Au-metallized coatings are represented by full symbols in Figure 7. For comparison, the KEDs of identical ions sputtered from molecular submonolayers adsorbed on gold are described by open symbols.

The first frame of Figure 7 shows the KEDs of Au-cationized Irganox molecules. Quite unexpectedly, the distributions match, indicating that the emission process is not significantly influenced by the different sample structures. The high-energy part of the distributions, slowly decaying and extending beyond 6−8 eV, is characteristic of cationized molecular ions, as observed in previous studies.[32,34] In contrast, the low-energy part, including negative apparent energies, is atypical. This negative-energy part of the distribution corresponds to ions formed in the acceleration section of the spectrometer, at some distance of the surface, either by some delayed ionization process or by unimolecular dissociation of larger aggregates in the vacuum. Both processes can be responsible for a kinetic energy deficit of the detected ions. The intensity measured for negative apparent energies is large, indicating the exceptional importance of such ion production channels for Irganox samples.

The energy spectra of cationized molecules sputtered from polystyrene are displayed in the second frame of Figure 7. For comparison, the energy spectra of $C_7H_7^+$ fragments are shown as an inset. The KEDs of $C_7H_7^+$ obtained from both surfaces merge. They are narrow, with a width at half-maximum close to 3 eV and a very steep intensity decrease beyond the distribution maximum. This shape has been explained using molecular dynamics simulations of the sputtering process.[35] The different absolute intensities of $C_7H_7^+$ measured for the two samples (Table 3) is probably due to an overall change of the ionization or the ion survival probability for this ion rather than a drastic change of the emission mechanism.

The distributions of Au-cationized polystyrene oligomers sputtered from both surfaces present the same distinctive features with respect to fingerprint fragments such as $C_7H_7^+$: a broader and asymmetric shape with a width exceeding 4 eV, a maximum between 2 and 4 eV, and a high-energy tail extending beyond 10 eV. One also notices a significant difference between the species sputtered from the Au-covered PS surface and those emitted from the submonolayer of PS on gold. The KED of quasimolecular ions sputtered from Au-covered surfaces are narrower and they exhibit a steeper high-energy tail. The low-energy parts of the distributions are slightly different too, with a larger intensity for the metallized PS sample.

To understand the different KED behaviors for PS and Irganox, it is reasonable to consider a different interaction of the Irganox and PS molecules with the gold clusters present at the surface. Our interpretation is that the distributions measured for metallized Irganox and Irganox cast on gold are identical because a major part of the signal may come from molecules covering the gold islands in the metallized sample, as a result of the diffusion of the antioxidant. Therefore, the nanoregions giving rise to cationized molecule emission might be similar in the two systems (Irganox molecules on top of a gold medium). Conversely, the dependence of the KEDs of Au-cationized PS molecules on the sample type is explained by the comparatively low diffusion coefficient of the 2-kDa PS oligomers, as observed elsewhere.[3] In other words, the detected signal would mainly originate from PS molecules *neighboring* gold islands but not necessarily from molecules *covering* the islands. With this assumption, the different KEDs of Au-cationized PS molecules would be the result of the different sputtering physics at play in the two systems. In a recent

(34) Delcorte, A.; Bertrand, P. *Surf. Sci.* **1998**, *412/413*, 97.
(35) Delcorte, A., Vanden Eynde, X., Bertrand, P., Vickerman, J. C., Garrison, B. J. *J. Phys. Chem. B* **2000**, *104*, 2673.

article modeling the kileelectronvolt particle-induced desorption of large molecules adsorbed on silver via molecular dynamics simulations,[36] it has been shown that cooperative motions in the metal sustrate—promoted with increasing primary beam energy—induce the ejection of molecules with a larger average kinetic versus internal energy ratio. As a result, the calculated KED of PS oligomers initially adsorbed on metal is broader for 5-keV bombardment than for 500-eV bombardment. In comparison, the interaction of kileelectronvolt projectiles with thick organic surface induces a significantly different physics, involving vibrational excitations, as indicated in ref 37. Therefore, the average internal energy transferred to the molecules in the ejection process might be comparatively higher and the kinetic energy of the surviving molecules comparatively lower.

For Irganox, the hypothesis of unimolecular decomposition reactions of large organometallic clusters giving rise to Au-cationized molecules is supported by the observation that clusters containing one molecule and one to five gold atoms are present in the positive secondary ion mass spectrum (Figure 3). A fraction of these (or larger) clusters sputtered from the sample surface could decompose after emission because of their relatively high internal energy and produce $(M + Au)^+$ complexes.[32]

Imaging SIMS. In the conclusion of our first article on Au metallization,[3] it was suggested that gold islands should also be beneficial for imaging applications because the characteristic size of the metal pattern on the surface is smaller than the best lateral resolution achieved in SIMS imaging at this point. Owing to the sensitivity enhancement and the cationization effect provided by the metal atoms, imaging on large (quasi)molecular ions should even be possible. This concept was tested using the kilodalton molecules selected for this study. A biaxially stretched PP film was chosen as a support for a "micropatterned" coating of PS oligomers. In this feasibility study, the PS coating pattern simply resulted from the drying of a PS-containing toluene droplet and its subsequent partial dewetting on the PP support.

Mass spectra and SIMS chemical mappings of the metallized sample are shown in Figure 8a−f. Because the nonmetallized PP film is a good insulator, its analysis by SIMS normally requires the use of a charge compensation device (electron floodgun). After gold evaporation, sample charging does not occur anymore. Therefore, the electron gun was not used for images b,c, e, and f. Another effect of the metallization procedure is that large PP chain segments, cationized by the metal, are observed in the secondary ion mass spectra.[3] The partial positive mass spectrum of Figure 8a shows this distribution of Au-cationized PP fragments, separated by a mass interval of 42 Da. Gold clusters are also detected at $m/z = 788$ (Au_4^+), $m/z = 985$ (Au_5^+), $m/z = 1182$ (Au_6^+), and $m/z = 1379$ (Au_7^+). Images b and c are related to ions that are characteristic of the PP substrate, $C_4H_9^+$ (Figure 8b) and the sum of Au-cationized PP chain segments in the range $988 < m/z < 1168$ (Figure 8c). In contrast, Figure 8d and images e and f correspond to characteristic signals of the PS oligomer distribution. The $C_7H_7^+$ ion (tropyllium, Figure 8e) is the most intense peak of the PS fingerprint ($0 < m/z < 200$). The image labeled AuPS+ (Figure 8f) sums up the intensities of a series of five Au-cationized PS oligomer peaks comprised between 1800 and 2300 Da (see Figure 8d). The three last images of Figure 8 have been obtained from a similar but nonmetallized sample, using the charge compensation setup and a larger analyzed area. The total ion image, the image of the butyl ion from PP, and the image of the $C_7H_7^+$ ion from PS are shown in Figure 8g−i, respectively. Quasimolecular ions are not observed in the mass spectrum of the pristine sample. The intensity range, represented by the number of counts per pixel, is indicated on every image. For some images where intensity is low (marked "conv"), an image treatment procedure has been used to increase the contrast; i.e., each pixel of the resulting image adds up the intensity of the eight surrounding pixels of the original image.

The complementary images collected from the metallized sample demonstrate very clearly that, in this region of the sample, the polystyrene oligomer coating forms stripes of 10−20-μm width. The two images corresponding to fingerprint fragment ions (Figure 8b and e) show high intensities and a good contrast. The images related to Au-cationized kilodalton molecules are less intense but they essentially provide the same information, with a much higher chemical selectivity. Indeed, in real-world samples, small hydrocarbon ions such as those used for image b and e could originate from undesirable hydrocarbon contamination.

In comparison, the images obtained from the pristine sample have a poor quality. Despite the use of an electron floodgun and the choice of a larger surface area for the bombardment ($180 \times 180\ \mu m^2$ instead of $120 \times 120\ \mu m^2$), the intensities are biased by sample charging effects; e.g., the top parts of the images are much darker than the bottom parts. Even after image treatment to improve the signal, the chemical contrast revealed by the image of the $C_7H_7^+$ fragments (PS) is almost absent from the image acquired from the butyl fragments (PP). On the pristine sample, the intensity per pixel for characteristic fragment ions rarely exceeds 3 counts before image treatment, that is ~20 times less than the intensity per pixel measured on the Au-covered sample. Finally, there is no useful signal in the mass spectrum beyond 200 Da, i.e., no (quasi)molecular ions.

This case study demonstrates that the metallization procedure significantly improves the quality of the chemical mappings obtained by SIMS imaging. The method promises to be particularly beneficial for insulating materials such as thick polymer films, beads, and industrial samples. In parallel, it has been shown elsewhere that polyatomic projectile beams are especially efficient for thick organic samples, in contrast with thin organic overlayers on inorganic substrates.[38−40] It is our belief that the combination of both techniques—polyatomic ion beams and sample surface metallization—should lead to a leap forward for molecular SIMS imaging sensitivity.

Comparison with Laser Ablation. In the course of this study, the question arose of whether metallic clusters might also operate as a matrix in laser ablation.[23,24] Indeed, it is expected that the clusters should absorb more UV radiation[41] and transfer the energy to the surrounding organic medium, possibly inducing molecular ejection. To check that possibility, Au-metallized mo-

(36) Delcorte, A.; Garrison, B. J. *J. Phys. Chem. B* **2000**, *104*, 6785.
(37) Delcorte, A.; Garrison, B. J. *J. Phys. Chem. B* **2003**, *107*, 2297.
(38) Gillen, G.; Roberson, S. *Rapid Commun. Mass Spectrom.* **1998**, *12*, 1303.
(39) Harris, R. D.; Baker, W. S.; Van Stipdonk, M. J.; Crooks, R. M.; Schweikert, E. A. *Rapid Commun. Mass Spectrom.* **1999**, *13*, 1374.
(40) Weibel, D.; Wong, S.; Lockyer, N.; Blenkinsopp, P.; Hill, R.; Vickerman, J. C. *Anal. Chem.* **2003**, *75*, 1754.
(41) Mafuné, F.; Kondow, T. *Chem. Phys. Lett.* **2003**, *372*, 199.

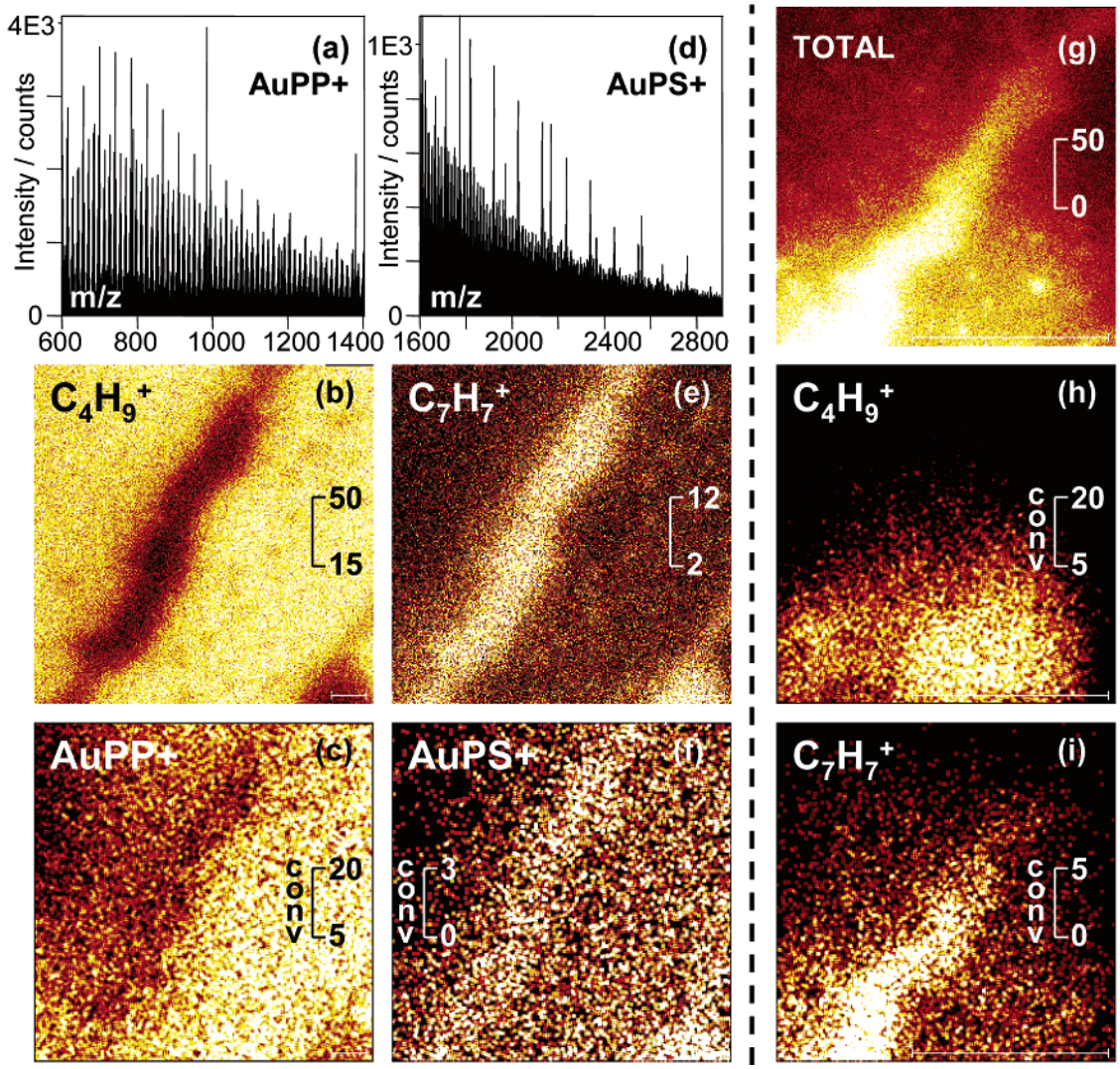

Figure 8. TOF-SIMS imaging on a polypropylene film locally covered by PS oligomers. The scale on each image indicates the lower (black) and upper (white) count-per-pixel limits used for the color coding. (a−f) Au-metallized sample (no charge compensation used); (g−i) pristine sample (use of a 20-eV electron floodgun). (a) Region of the mass spectrum showing the distribution of Au-cationized PP chain segments; (b) 120 × 120 μm^2 image of the butyl fragments of PP; (c) 120 × 120 μm^2 image of the Au-cationized chain segments of PP; (d) region of the mass spectrum showing the distribution of Au-cationized PS oligomers; (e) 120 × 120 μm^2 image of the $C_7H_7^+$ fragments of PS; (f) 120 × 120 μm^2 image of the Au-cationized PS oligomers; (g) total ion image obtained from the nonmetallized sample; (h) 180 × 180 μm^2 image of the butyl fragments of PP; (i) 180 × 180 μm^2 image of the $C_7H_7^+$ fragments of PS.

lecular coatings were analyzed by LAMS, using a UV laser (337 nm).

First, Irganox and polystyrene were characterized under MALDI conditions, using the sample preparation procedure described by Hanton and co-workers.[42] This procedure involves the use of dithranol as a matrix and of silver trifluoroacetate as a cationizing agent. The high-mass range of the MALDI spectrum of PS is shown in Figure 9. The distribution of silver-cationized PS oligomers is observed with a good signal-to-noise ratio. As usual in MALDI, however, the characteristic fragments of the analyte in the lower mass range of the spectrum (not shown) are masked by the signals related to the matrix and moreover, in this particular case, to the trifluoroacetate cationizing agent.

The positive LA mass spectrum corresponding to the Au-cationized polystyrene oligomer coating is shown in Figure 10. In contrast with the SIMS and the MALDI spectra (Figure 9), the high-mass range of the LA spectrum (Figure 10, first frame) does not show any sign of intact Au-cationized molecules. Only positively charged gold clusters, and especially those containing an odd number of atoms, are detected between 1000 and 3000 Da, where cationized polystyrene oligomers are expected (Figure 9). In the same manner, measurements conducted with a metallized Irganox sample do not lead to the detection of Irganox molecular ions. Therefore, the metallization procedure, used as such, does not result in the emission of cationized intact molecules under 337-nm laser irradiation. Nevertheless, in the low-mass range (second frame), besides intense Na^+ and K^+ peaks, the characteristic fragments of polystyrene ($C_7H_7^+$, $C_8H_9^+$, $C_9H_7^+$, $C_9H_9^+$, $C_{15}H_{13}^+$) dominate the spectrum. The nature of the observed fragments and even their relative intensities strongly remind the SIMS spectrum of similar polystyrene samples.[3] In

(42) Hanton, S. D.; Cornelio Clark, P. A.; Owens, K. G. *J. Am. Soc. Mass Spectrom.* **1999**, *10*, 104.

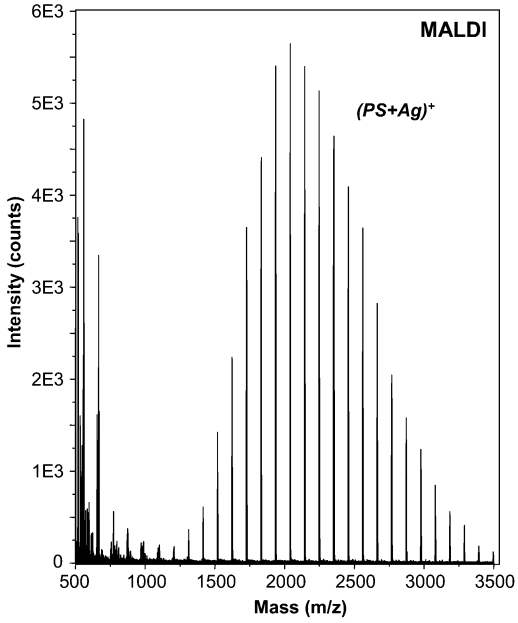

Figure 9. MALDI mass spectrum (100 laser shots) of an overlayer of polystyrene on a primer layer of dithranol and silver trifluoroacetate.

LAMS, these characteristic fragments are also observed for a similar power density under 193-nm irradiation (absorption maximum) of pristine PS, but not under 355-nm irradiation (similar absorption as 337 nm).[43] The detailed analysis of the LA mass spectrum of Au-covered PS oligomers also shows that the laser induces the desorption of Au-cationized *fragments*. Between 200 and 600 Da, positively charged organometallic complexes are detected (Figure 10, third frame), among which $AuC_8H_8^+$ (PS monomer), $AuC_{15}H_{15}^+$, $AuC_{16}H_{16}^+$ (PS dimer), and $AuC_{24}H_{24}^+$ (PS trimer). These peaks indicate that the recombination of an Au atom with an organic fragment to form a positively charged complex occurs in laser ablation. For comparison, the corresponding TOF-SIMS spectrum is presented in the bottom frame of Figure 10. It demonstrates the striking resemblance between the SIMS and LAMS results in this mass range.

In practice, the useful role of Au clusters or islands as photon absorbers in LA was also confirmed using a thick polyolefin sample (polypropylene). While no desorbed ion signal was measured under 337-nm laser irradiation of pristine PP samples, we detected the detailed fragmentation pattern of PP in the mass range $0 < m/z < 200$ for thick samples metallized using the conditions described in the Experimental Section.

From the fundamental viewpoint, the thermal effect accompanying the high absorbance of Au clusters may contribute to explain the absence of intact cationized molecules in the LA mass spectrum of Au-covered polystyrene and Irganox samples. Indeed, it is known that photochemical and thermal processes occur simultaneously during laser irradiation. The thermal conductivity of gold is high (3.18 $W \cdot cm^{-1} \cdot K^{-1}$ at room temperature); consequently, the heat transfer from the irradiated clusters to the surrounding organic medium should be important. This heating might be sufficient to induce thermal degradation or thermal depolymerization, thereby accounting for the absence of intact Au-cationized molecules in the mass spectra.[43] In turn, thermal

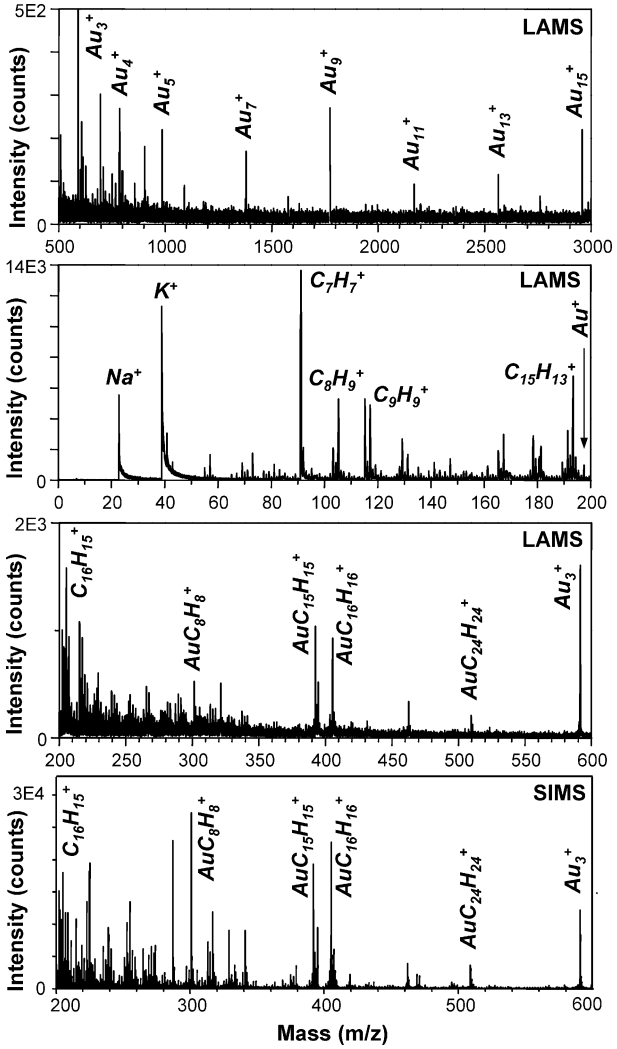

Figure 10. Laser ablation mass spectrum (30 laser shots) of a metallized polystyrene oligomer film (frames 1−3). The last frame shows the intermediate mass region ($200 < m/z < 600$) of the SIMS spectrum of an identical sample.

degradation is expected to produce small organic fragments. After ejection, these fragments can be involved in various gas-phase processes, among which the interaction with ejected gold atoms or clusters, possibly inducing Au cationization. On the other hand, we cannot totally exclude that the absence of intact Au-cationized molecules could be due to specific processes affecting ionization under LA conditions, e.g., a low ionization probability of molecule−metal complexes, the collision-induced dissociation of such complexes, or their preferential neutralization in the ejected plume. Because of the density of the plume, charge exchange between cationized molecules and neutral gold clusters/hydrocarbon molecules is likely to occur.

Finally, previous reports may help us understand the actual formation process of Au-cationized species, including the small cationized fragments observed in both SIMS and LAMS experiments. In their study of polyethylene, Jeong et al. demonstrated that bare Au^+ ions do not react with hydrocarbons to generate Au-cationized species.[44] Instead, the association of excited neutral

(43) Ruch, D. Ph.D. Thesis, University of Metz, 2002.

(44) Jeong, S.; Fisher, K. J.; Howe, R. F.; Wilett, G. D. *Microporous Mater.* **1998**, *22*, 369.

gold atoms with organic fragments could, after the emission of a thermal electron, generate organometallic ions, as was proposed by Wojciechowski et al.[45] In LAMS, the higher sample absorbance induced by the gold clusters and its subsequent heating also lead to an increased gas-phase density, which should favor such collision-induced processes.

CONCLUSION

Recently, gold metallization has proven to be an efficient route to enhance fragment and molecular ion yields in SIMS of organic samples, including polymers. In the present study, our attention has been focused on the enhanced desorption of kilodalton (quasi)molecular ions from organic films of Irganox, polystyrene, polyalanine, and copper phthalocyanine covered with a small amount of metal (Ag, Au). The metallized films were directly compared to pristine coatings and to organic submonolayers on silver and gold. The main observations are the following:

The results are sample dependent: while intense peaks of metal-cationized molecules are detected in the mass spectra of Irganox and PS, no metal cationization occurs for polyalanine and copper phthalocyanine. In the latter case, the absence of cationization by the evaporated metal might be related to the copper atom already present at the center of the molecule. For Irganox, the intensity of the cationized molecule induced by metallization is more than 2 orders of magnitude larger than the intensity of the molecular ion sputtered from the pristine sample (enhancement factor 660 for Au metallization and 450 for Ag metallization).

In general, the intensity of fragment and molecular ions that are *not* the result of metal cationization is also enhanced by the metallization procedure. The enhancement factor is usually comprised between 1 and 10 for short fragments. Under gold metallization, the enhancement factor is close to 30 for the molecular ion of Irganox and for the 9-mer of alanine.

Ion beam degradation studies indicate that the decay of the quasimolecular ion signals is not strongly dependent on the sample preparation procedure. All the damage cross sections (σ) are comprised between 10^{-13} and 10^{-12} cm^2, with a maximum degradation for polystyrene cast as a submonolayer on silver ($\sigma = 4.2 \times 10^{-13}$ cm^2) and a minimum degradation for polystyrene and Irganox films covered with gold ($\sigma = 2.4 \times 10^{-13}$ cm^2).

The kinetic energy distributions of Au-cationized Irganox molecules sputtered from metallized films and from submonolayers on metal are almost identical. They indicate a similar desorption mechanism and, possibly, the migration of Irganox molecules on the metal islands in the case of the metallized film. The large number of ions detected with an energy deficit shows the importance of delayed ion formation in the vacuum. The presence of larger $(M + Au_x)^+$ $(1 < x \leq 5)$ clusters in the mass spectrum points to the unimolecular dissociation of such clusters as a source of Au-cationized Irganox molecules. In contrast, the energy distributions of Au-cationized PS oligomers depend on the preparation procedure, suggesting slightly different desorption/ionization processes. These distributions also contain much less ions with an energy deficit.

The metallization procedure constitutes an excellent way of increasing sensitivity for SIMS imaging of thick organic samples. High intensities of fingerprint fragments lead to high-quality images even for insulators, and (quasi)molecular ion imaging provides the desired chemical selectivity. There is no doubt that the combined use of sample metallization and polyatomic primary ion beams (Au_n^+, $C60^+$) will greatly enhance the capability of SIMS for large molecular ion imaging.

Finally, no cationized molecular ions are detected when Au-metallized Irganox and polystyrene samples are irradiated with a 337-nm laser in a laser ablation experiment. Nevertheless, small cationized fragments, up to the trimer for PS, are observed in the positive mass spectrum, demonstrating the possibility of metal cationization for such samples in LAMS. The use of gold clusters also enhances the intensity of PS fingerprint fragments, which are usually not detected for pristine PS using these conditions of laser wavelength and fluence. In comparison, the use of a MALDI matrix combined to a Ag-containing cationizing agent gives rise to the silver-cationized PS oligomer distribution, but the fingerprint region of the spectrum is not interpretable because of the interference between the matrix, the cationizing agent, and the PS peaks.

ACKNOWLEDGMENT

A.D. acknowledges the financial support of the Belgian Fonds National pour la Recherche Scientifique. This work is also supported by the Interuniversity Attraction Pole program on "Quantum sized effects in nanostructured materials" of the Belgian Federal State. The ToF-SIMS equipment was acquired with the support of the Région Wallonne and FRFC-Loterie Nationale of Belgium.

Received for review May 22, 2003. Accepted September 4, 2003.

AC0302105

(45) Wocjiechowski, I.; Delcorte, A.; Gonze, X.; Bertrand, P.; *Chem. Phys. Lett.* **2001**, *346*, 1.